Two-body decays of B mesons

R. Giles, J. Hassard, M. Hempstead, K. Kinoshita, W. W. MacKay, F. M. Pipkin, and Richard Wilson
Harvard University, Cambridge, Massachusetts 02138

P. Haas, T. Jensen, H. Kagan, and R. Kass
Ohio State University, Columbus, Ohio, 43210

S. Behrends, K. Chadwick, J. Chauveau,* T. Gentile, Jan M. Guida, Joan A. Guida, A. C. Melissinos, S. L. Olsen, G. Parkhurst, D. Peterson, R. Poling, C. Rosenfeld, E. H. Thorndike, and P. Tipton
University of Rochester, Rochester, New York 14627

D. Besson, J. Green, R. Namjoshi, F. Sannes, P. Skubic,† A. Snyder,‡ and R. Stone
Rutgers University, New Brunswick, New Jersey 08854

A. Chen, M. Goldberg, M. E. Hejazifar, N. Horwitz, A. Jawahery, P. Lipari, G. C. Moneti, C. G. Trahern, and H. van Hecke
Syracuse University, Syracuse, New York 13210

M. S. Alam, S. E. Csorna, L. Garren, M. D. Mestayer, R. S. Panvini, and Xia Yi
Vanderbilt University, Nashville, Tennessee 37235

P. Avery, C. Bebek, K. Berkelman, D. G. Cassel, J. W. DeWire, R. Ehrlich, T. Ferguson, R. Galik, M. G. D. Gilchriese, B. Gittelman, M. Halling, D. L. Hartill, S. Holzner, M. Ito, J. Kandaswamy, D. L. Kreinick, Y. Kubota, N. B. Mistry, F. Morrow, E. Nordberg, M. Ogg, K. Read, A. Silverman, P. C. Stein, S. Stone, R. Wilcke,§ and Xu Kezun
Cornell University, Ithaca, New York 14853

A. J. Sadoff
Ithaca College, Ithaca, New York 14850

(Received 8 June 1984; revised manuscript received 10 September 1984)

Various exclusive and inclusive decays of B mesons have been studied using data taken with the CLEO detector at the Cornell Electron Storage Ring. The exclusive modes examined are mostly decays into two hadrons. The branching ratio for a B meson to decay into a charmed meson and a charged pion is found to be about 2%. Upper limits are quoted for other final states ψK^-, $\pi^+\pi^-$, $\rho^0\pi^-$, $\mu^+\mu^-$, e^+e^-, and $\mu^\pm e^\mp$. We also give an upper limit on inclusive ψ production and improved charged multiplicity measurements.

I. INTRODUCTION

Weak decays of B mesons provide a unique testing ground for both electroweak theory and quantum chromodynamics (QCD). B mesons are composed of a $\bar{b}$ antiquark and a light quark, either a d (B^0) or a u (B^+). In the standard electroweak model[1] the b quark can decay into the c quark or the u quark by emitting a virtual intermediate vector boson. The possible decay schemes[2] of $\bar{B}^0$ and B^- are shown in Fig. 1 for both the $b\to c$ and $b\to u$ cases. In the "spectator" diagrams the B meson decays when the b quark decays. In the "annihilation" and "exchange" diagrams the light antiquark is directly involved in the decay of the heavy meson. Since measurements, made at the Cornell Electron Storage Ring, of the shape of the lepton spectrum from B decays[3] have limited the ratio of branching fractions of $b\to u/b\to c$ to be $<4\%$ at 90% confidence level, a charmed particle should be present in almost all B-meson decays.

Even if we assume that the spectator model (Fig. 1) describes B decay, there are still many possible ways to describe how hadrons might form. In one model, the four final-state primary partons interact with each other without regard to color or charge and produce hadron states proportional to the available phase space. An alternative model is based on the fact that QCD requires hadrons to be color singlets. In this model, which we call the "spectator model without color mixing," the quarks from the W may mix with the other quarks only when they have the same color as the initial b quark (Fig. 2). The amount of this mixing can be measured by examining inclusive ψ production from B decay, which will be discussed in this paper. The spectator-antiquark and charmed-quark system, minimally, gives rise to a D

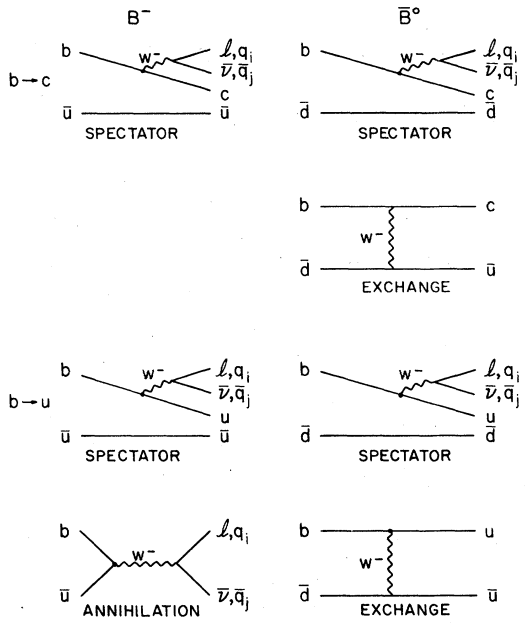

FIG. 1. Decay diagrams for $\bar{B}^0$ and B^- mesons.

meson, but can also create additional quark-antiquark pairs from the vacuum and so produce additional hadrons. We will show that measurements of the D^0 momentum spectrum and charged multiplicity in B decay imply that the average number of additional hadrons produced from the spectator and charmed quarks is small and consistent with zero.

The large mass of the B meson makes the expected number of low-multiplicity decays relatively small. Nevertheless such decays have been found, involving a D meson and one or two charged pions.[4] Two-body decays of B mesons test both the underlying electroweak quark-decay mechanisms and additional corrections imposed by QCD. In Sec. III of this paper, we report on several different measurements of the $B\to D\pi^{\mp}$ branching fractions. We also give upper limits on other two-body B-meson decays: one containing hidden charm, $B^-\to\psi K^-$ in Sec. II C, and two which could result from the $b\to u$ transition, $B^0\to\pi^+\pi^-$, and $B^-\to\rho^0\pi^-$, and their charge conjugates in Sec. IV. In this work, the specification of a particular reaction also implies its charge conjugate. Also, in Sec. IV, we set limits on exclusive B^0 decay into two charged leptons.

The B mesons considered here have been produced in $\Upsilon(4S)$ decays at the Cornell Electron Storage Ring (CESR),[5] and the data were accumulated with the CLEO detector. As the CLEO detector has been described in detail elsewhere,[6] we give only a brief description here. The central region of the detector contains a beam-pipe proportional chamber and a cylindrical drift chamber centered inside a superconducting solenoidal magnet of 1-m radius operating at 1.0 T. Outside the coil are eight identical sectors of particle-identification apparatus. Each sector consists of a three-layer planar drift chamber closest to the magnet coil, a pressurized proportional-wire-chamber system capable of measuring specific ionization (dE/dx), an array of twelve time-of-flight scintillation counters, and, furthest from the intersection point, a 44-layer lead and proportional-tube shower chamber. The eight sectors are followed by 0.5 to 1.0 m of iron, and finally there is a two-dimensional array of planar drift chambers for muon identification, with additional drift chambers interspersed within the iron to allow identification of lower-momentum muons.

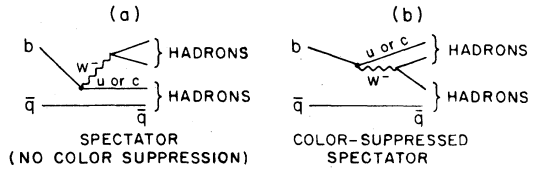

FIG. 2. Spectator diagrams for b-quark decay without (a) and with (b) color suppression. The diagram with color suppression is only one of several such diagrams.

The detector excels at reconstructing final states consisting of only charged particles, since the efficiency for finding a charged track is high (85%) and the momentum resolution is good. For tracks which are not limited by multiple scattering, the rms spread in momentum is given approximately as $\delta p/p=0.012p$ (p in GeV/c). Neutral pions, on the other hand, are not well measured and the detector has poor efficiency for finding them.

A total integrated luminosity of 40.6 pb^{-1} was accumulated at the $\Upsilon(4S)$ resonance and 17.1 pb^{-1} was accumulated in the continuum region between the $\Upsilon(3S)$ and $\Upsilon(4S)$ resonances. We accepted hadronic events according to the following rules.

(1) Each event must have at least five charged tracks found in the drift chamber.

(2) There must be a common track vertex lying within ± 8 cm of the nominal interaction point along the beam line and within ± 2 cm transverse to the beam line.

(3) At least 250 MeV of electromagnetic energy must be detected in the shower detectors.

(4) At least 30% of the center-of-mass energy must be visible as charged tracks in the drift chamber.

The electromagnetic-energy cut was chosen to suppress beam-pipe interactions; the charged-energy cut removes two-photon collision events; and the multiplicity cut reduces $\tau^+\tau^-$ background. The acceptance for $\Upsilon(4S)$ events is 86.3%, and for continuum two-jet events is 70.1%. τ pairs pass these cuts at a 15.1% level.

After applying these cuts we had 42 000 $B\bar{B}$ events and 106 000 continuum events on the $\Upsilon(4S)$ and a separate sample of 45 000 continuum events.

II. INCLUSIVE PROPERTIES

A. D^0 momentum spectrum

We have previously reported a measurement of the momentum spectrum of D^0 mesons resulting from B-meson decay[7] (Fig. 3). The spectrum peaks at large momentum and appears similar to the spectrum expected for the semileptonic decay of a B meson to the spectrum expected for the semileptonic decay of a B meson to a D meson (solid curve in Fig. 3). This curve is the result of a calculation for the process $b\to ce^-\bar{\nu}_e$ in which the b quark is given the mass of the B meson and the c quark

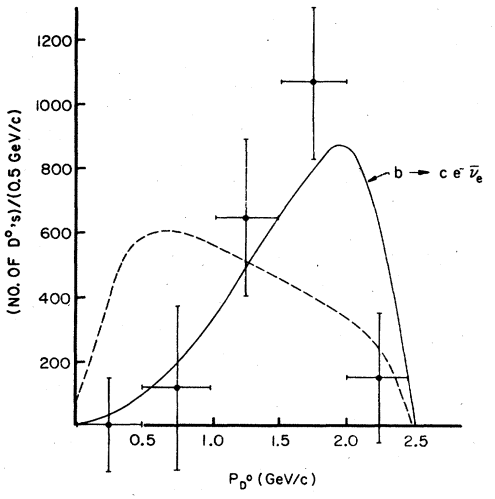

FIG. 3. D^0 momentum distribution from B-meson decay. The solid curve is the theoretical expectation for the semileptonic decay $b \to c e^- \bar{\nu}_e$, in which the decay proceeds via $V-A$. The dashed curve is the result of a phase-space model (see text).

the mass of the D^0 meson.[8] The other curve in Fig. 3 results from a model in which the four quarks are allowed to interact with each other at random and produce final-state hadrons distributed according to phase space. This curve is in disagreement with the data, even though the model which produced it agrees with all other inclusive properties, including the charged multiplicity distribution and the inclusive momentum spectrum. In the spectator model without color mixing, final-state hadrons arise from quark-antiquark creation in the c-quark-plus-spectator-antiquark system, in the D decay, and in the quark-antiquark system formed from the W^-. That is, the similarity of the D^0 momentum spectrum in all B decays to the prediction for semileptonic decays suggests that most B decays follow the same decay scheme as the semileptonics, namely, the spectator model without color mixing.

B. Charged multiplicity

The comparison between the mean charged multiplicity in semileptonic B decay and the mean charged multiplicity in D decay gives information about particle creation in the c-quark-plus-spectator ($c\bar{u}$ or $c\bar{d}$) hadronization. We have made new measurements of the charged multiplicity with the entire data sample. The analysis technique was the same as used previously,[9] and yields an average charged multiplicity in $B\bar{B}$ events of $10.99\pm0.06\pm0.29$ with a dispersion (the root-mean-square spread of the distribution) of $3.08\pm0.04\pm0.19$. The first error quoted is statistical and the second systematic. Whenever two errors are quoted in this work, they follow this form. For events with one or more identified leptons the average charged multiplicity is $9.30\pm0.10\pm0.33$ with a dispersion of $2.23\pm0.10\pm0.23$. We can unfold the average charged multiplicity purely in hadronic B decay and in semileptonic B decay by using the measured B semileptonic branching ratio of $11.4\pm0.7\%$.[3] We find the charged multiplicity in a hadronic B decay is 6.0 ± 0.3, and for semileptonic decays is 3.8 ± 0.4, where we have added the systematic and statistical errors in quadrature.[18]

To proceed further we make two assumptions about semileptonic B decay. First we take $(b\to c)/(b\to \text{all})$ to be 100%. Second, we assume that an equal mixture of D and D^* is produced. These assumptions are consistent with the lepton momentum spectrum in B decay from which we have determined that $(b\to c)/(b\to \text{all}) > 96\%$ at 90% confidence level.[3] In an equal mixture of D and D^* decaying, the measured charged multiplicity is 2.52 ± 0.11 (Ref. 17). Since the lepton itself gives one unit of charged multiplicity, the remaining unaccounted charged multiplicity of X is 0.3 ± 0.4 units for B decaying into (D or D^*)$l\nu X$. This is consistent with there being little or no fragmentation of the c quark and the spectator antiquark into additional particles X in semileptonic B decay.

C. ψ production

The b-decay Hamiltonian may be separated into color-singlet and color-octet components. The color-octet part leads to the decay diagram shown in Fig. 2(b), where the colors of the initial b quark and the quarks from the W are the same. The ψ contains hidden charm (a $c\bar{c}$ pair) and can be made in B decay through the color-suppressed spectator diagram (Fig. 4). This was first discussed by Fritzsch,[11] and later by Kühn, Nussinov, and Rückl, by DeGrand and Toussaint, and by Wise.[12] This decay occurs only when the virtual W^- decays into a $\bar{c}s$ pair, which happens, according to phase-space calculations, about 15% of the time. The color of the $\bar{c}$ must be the same as that of the original b quark. This happens $\frac{1}{3}$ of the time in the amplitude, thus reducing the probability by a factor of 9. Multiplying these factors gives an estimate of the branching fraction of 1.7%. Additional QCD corrections[13] could lower this value. We search for ψ's in their e^+e^- and $\mu^+\mu^-$ decay modes. Electrons are identified by using both dE/dx and shower measurements. Muons are identified by the planar drift chambers outside 0.5 to 1.0 m of iron. The electron and muon identification procedures have been described elsewhere.[14]

There were 42 events at the $\Upsilon(4S)$ which had two identified muons. The dimuon mass distribution of masses above 2.5 GeV is shown in Fig. 5. There is a small excess of events at the ψ mass. The background consists of events with both a B and a $\bar{B}$ decaying semileptonically, events with one semileptonic decay and an oppositely charged hadron faking a muon, and events with two oppositely charged hadrons both faking muons. The mass distribution of this background has been determined by pairing an apparent muon from one candidate dimuon event with the muons from all other dimuon events. The background determined in this way and normalized in the mass interval 2.500 to 2.945 and 3.245 to 4.000 GeV is

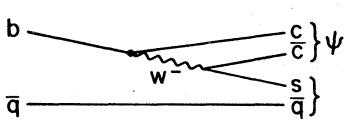

FIG. 4. Mechanism of ψ production through the color-suppressed spectator diagram.

shown as the dashed curve in Fig. 5.

We accept as ψ candidates muon pairs which have masses within 1.5 standard deviations of the ψ mass. The rms mass resolution of 60 MeV has been determined by Monte Carlo simulation. There are six pairs within this interval, with an estimated background contribution of 2.3 ± 0.5. The efficiency for detecting $B\to\psi+$ anything by this procedure is the product of five factors. (1) the geometrical and momentum acceptance for the muon pair as determined by the iron thickness (0.18), (2) the square of track-fitting efficiency (0.85^2), (3) the square of the detection efficiency for the planar drift chambers (0.87^2), (4) the fraction of dimuon ψ decays which satisfy the selection criteria (0.87), and (5) the branching ratio for the decay[7] $\psi\to\mu^+\mu^-$ (0.074). The overall efficiency is 0.0063 ± 0.0019.

To look inclusively for ψ's which decayed to e^+e^-, we required that at least one electron be identified. Mass combinations were formed by pairing the identified electron with all oppositely charged particles in the event. A combination was subsequently discarded if it could be shown by dE/dx or shower measurements that the second track was not an electron. We retained particles for which no unambiguous determination could be made, either because they were outside the electron identification fiducial volume, or because dE/dx and shower measurements were inconclusive. The mass distribution for electron pairs selected in this way is shown in Fig. 6(a). Again a weak signal appears at the ψ mass. The mass resolution for this case is poorer than for $\psi\to\mu^+\mu^-$ because of radiation of the electrons in the 5%-radiation-length-thick beam pipe and inner proportional chamber. In Fig. 6(b) we show those events from Fig. 6(a) in which the second track of the ψ has been tagged as being a likely electron either by dE/dx or by shower criteria. There seems to be a clustering of events near the ψ mass.

The background for dielectrons consists of the same three components as that for dimuons. Since positive identification is required of only one electron, however,

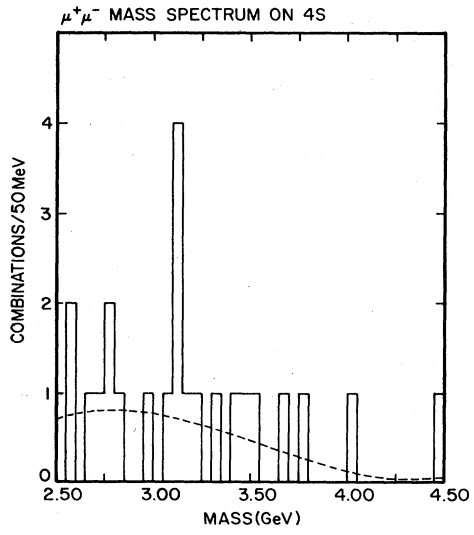

FIG. 5. Dimuon mass distribution for $\Upsilon(4S)$ events. Both muons are positively identified.

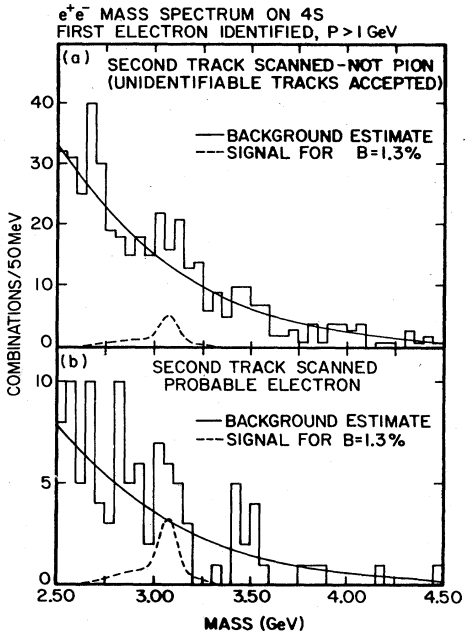

FIG. 6. Dielectron mass distribution for $\Upsilon(4S)$ events. (a) One electron is identified and the second is required to be inconsistent with a pion hypothesis if it strikes a sensitive region of the detector. (b) Both electrons are identified.

the fake and double-fake components are more important. The background has been estimated by the same procedure as for muons. An identified electron was taken from one event and substituted for an identified electron of the same sign in a second event. No identification requirement was imposed on the particles in the second event which were paired with the electron. The background was normalized to have the same area as the data in the mass interval 2.500 to 2.845 and 3.245 to 4.500 GeV. In Fig. 6 the background and the contribution from $B\to\psi X$ with a 1.3% branching ratio are shown as solid and dashed curves, respectively.

The efficiency ϵ_ψ for detecting a ψ through the decay $\psi\to e^+e^-$ is determined from our efficiency ϵ_1 for identifying an electron and from ϵ_2 for simply finding the second track, through the formula

$$\epsilon_\psi=[(2\epsilon_1(1-\epsilon_1)\epsilon_2+\epsilon_1^2]B(\psi\to e^+e^-)\ .$$

With our values for ϵ_1 and ϵ_2 (0.24 ± 0.01 and 0.80 ± 0.04, respectively),[14] we find $\epsilon_\psi=0.026$. We have fitted the data in Fig. 6(a) to the background shape determined as described above, plus a signal shape determined by a Monte Carlo calculation which included momentum smearing due to the finite resolution of the cylindrical drift chamber and radiation in the beam pipe and inner proportional chamber. In the three mass bins from 2.945 to 3.145 GeV there are a total of 59 ψ candidates with an expected background of 40, implying a total of 19 ± 8 ψ events. We correct this number by ϵ_ψ and the 67% probability for the dielectron to fall in this restricted mass interval.

The muon and electron results are consistent with each other and may be combined to give a $B\to\psi X$ branching-

ratio upper limit of 1.6% (90% confidence). If the signal were real it would correspond to a branching ratio of $(1.0^{+0.5}_{-0.4})\%$ for $B\to\psi X$. This small upper limit indicates that color suppression may be an important factor in B decay.

In the foregoing discussion we have assumed that all ψ production which we observe comes from B-meson decay. We have tested the assumption that no ψ's are produced in the continuum by searching for ψ's in the 17.1 pb^{-1} of data collected between the $\Upsilon(3S)$ and $\Upsilon(4S)$. It should be noted that a major potential source of ψ background, high-energy leptons from semileptonic B decay, is absent for continuum events. There is only one opposite-sign dimuon observed in this continuum data sample and it has a mass far below that of the ψ. The dielectron mass spectrum for these data is shown in Fig. 7. The background in Fig. 7 has been calculated by the same substitution procedure as that of Fig. 6. From the electron data of Fig. 7 and the absence of any dimuon candidates we obtain a 90% confidence level upper limit for continuum ψ production of 0.005 per event. Thus the misinterpretation of continuum ψ production at the $\Upsilon(4S)$ would lead to an apparent branching ratio for $B\to\psi X$ of less than 0.3% with 90% confidence.

We have also searched for evidence of the exclusive decays $B^-\to\psi K^-$ and $\bar{B}^0\to\psi K^-\pi^+$. For this search we expanded our muon sample to include events with just one identified muon. For each of these events, the muon was paired with all oppositely charged tracks. This procedure increases efficiency at the expense of significantly worsened background in the ψ sample. For the electrons, we used the event sample shown in Fig. 6(a). We selected muon combinations with masses within 0.150 GeV of the ψ mass and electron combinations in the mass interval 2.845 to 3.245 GeV. Events with satisfactory combinations were subjected to kinematic fits constraining the energy of the B-meson candidates to the beam energy and the mass of the lepton pair to the ψ mass. We kept all events with $\chi^2<14$ (based on a Monte Carlo study) and examined the fitted invariant masses to see if they were consistent with the known B mass of 5.272 GeV.[4] We found one candidate for ψK^- and two candidates for $\psi K^-\pi^+$, leading to 90%-confidence-level upper limits for the branching ratio of 0.26% and 0.63%, respectively.

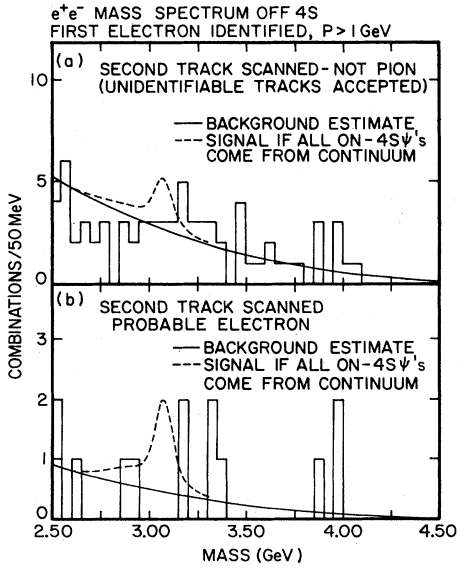

FIG. 7. Dielectron mass distribution for continuum events. (a) One electron is identified and the second is required to be inconsistent with a pion hypothesis if it strikes a sensitive region of the detector. (b) Both electrons are identified.

III. $B\to D\pi^-$

A. Introduction

If the spectator model without color mixing does indeed describe B decay, then two-body decay into $D\pi$ would occur when the virtual W^- materializes as a π^- meson. However, for $\bar{B}^0$ decay into D^+ (or D^{*+})π^-, both the spectator and exchange diagrams (Fig. 8), are possible. For $B^-\to D^0(D^{*0})\pi^-$, only the spectator diagram applies.

From our previously measured[4] B mass and the mass of the $\Upsilon(4S)$, the momentum of the B mesons resulting from the $\Upsilon(4S)$ decay is determined to be approximately 400 MeV/c. The B mesons are thus moving very slowly in the laboratory system with $\beta=0.08$. If the B's were at rest, two-body decays into $D\pi$ would produce monochromatic D's and π's. The motion of the B's somewhat broadens these spectra. Since the D decays into many particles, it is easier to look for direct evidence of the accompanying π^-.

B. Single-particle momentum spectrum

Figure 9(a) shows the charged-particle momentum spectrum (in $x=p/E_{\rm beam}$) from the $\Upsilon(4S)$ with the continuum contribution subtracted. Charged tracks close to the beam direction, with absolute value of the cosine of the dip angle less than 0.8, have been eliminated. The distribution goes to zero near an x value of 0.5 because the $\Upsilon(4S)$ decays into a $B\bar{B}$ pair and each B has half the energy of the $\Upsilon(4S)$. The shoulder at large x is partially due to leptons from semileptonic B decay. In addition, decays of D mesons which have themselves come from B decay give charged particles at large x. The lepton spectrum has been well measured[3] and the yields from D's have been simulated by Monte Carlo [Fig. 9(b)]. We subtract these spectra from the x distribution, giving the particle spectrum shown in Fig. 9(c). The remarkable feature of this distribution is the rather prominent bump at x values above 0.4. Pion spectra from Monte Carlo simulations of the process $B\to Dn\pi$ ($n=1,\ldots,4$) are shown in Fig. 10.

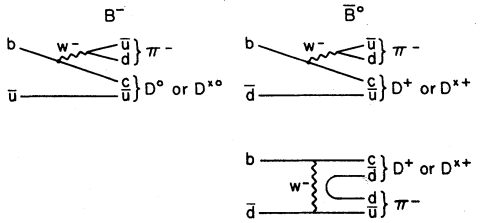

FIG. 8. Diagram for two-body decay of $\bar{B}^0$ and B^- mesons into a charmed meson and a charged pion.

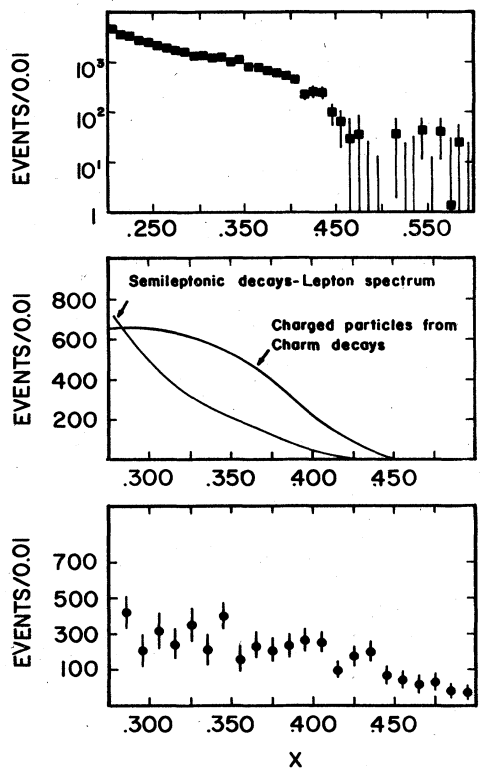

FIG. 9. Charged-particle x distribution from B-meson decays. (a) All charged tracks within restricted angular interval. (b) Spectra for leptons from semileptonic B decay and charged tracks from charm decays. (c) Charged-particle spectrum with leptons and charm decay products subtracted.

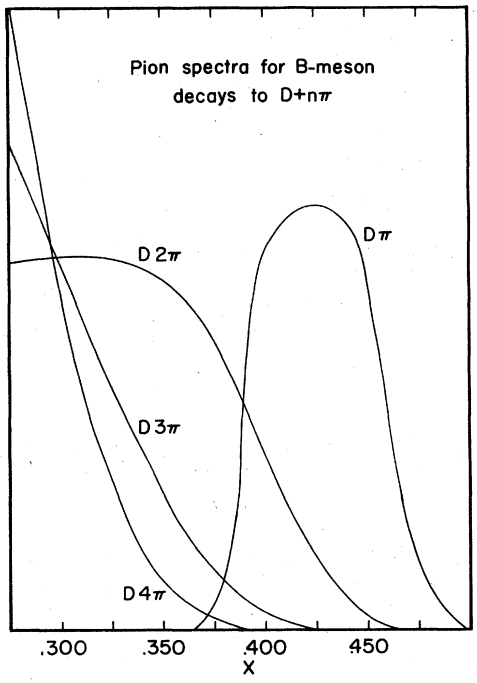

FIG. 10. Monte Carlo—simulated x distributions for the processes $B\to Dn\pi$ ($n=1,\ldots,4$).

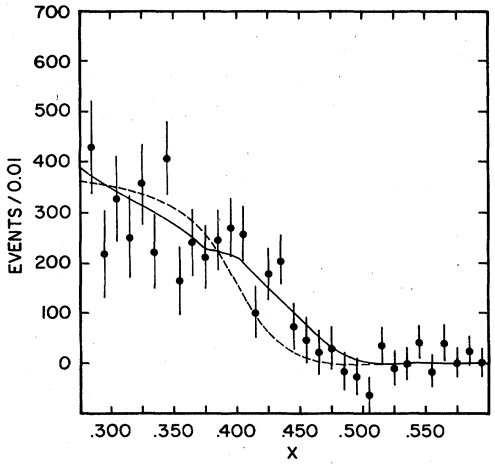

FIG. 11. Lepton-subtracted x distribution fitted to the four processes $B\to Dn\pi$ ($n=1,\ldots 4$) (solid curve), and to three of the processes excluding the $n=1$ reaction (dashed curve).

Pions from the channel $B\to D\pi$ appear as a narrow bump centered at x equals 0.42. Whether there is a D or D^* in the final state has little effect on the pion momentum. Figure 11 shows the x distribution above an x of 0.25 fitted to a linear combination of all four Monte Carlo spectra. The $D\pi$ component contains 670 ± 200 events. We have also fitted the distribution excluding the $B\to D\pi$ component (dashed line in Fig. 11). The χ^2 per degree of freedom is 21.7/19 with the $D\pi$ component included and 43.1/20 with it absent. Clearly, the $D\pi$ component is necessary to explain the data.

The number of $D\pi$ events found this way can be converted to a branching fraction for the sum of all reactions in which a B decays into a D and a charged pion. The possible reactions are

$$B^-\to D^0\pi^-\ , \tag{1}$$

$$B^-\to D^{*0}\pi^-\ , \tag{2}$$

$$\bar{B}^0\to D^+\pi^-\ , \tag{3}$$

$$\bar{B}^0\to D^{*+}\pi^-\ . \tag{4}$$

We have determined the efficiency to find a charged pion in the restricted angular range to be $(83\pm3)\%$. We find a branching fraction of $(2.0\pm0.6)\%$ for the sum of reactions (1) through (4). The systematic errors include errors in the continuum subtraction ($\pm0.4\%$), in the relative amount of $D^0\pi$ and $D^*\pi$ ($\pm0.1\%$), in the $D2\pi$ matrix element[15] ($\pm0.1\%$), and in the efficiency to find the π^- ($\pm0.1\%$). Negligible errors result from uncertainties on the B mass, the semileptonic branching fraction, and the spectrum of charged particles from charm decays. The total systematic error is then $\pm0.5\%$.

C. Slow-pion–fast-pion correlation

Several kinematic properties of the decay

$$\bar{B}^0\to D^{*+}\pi^-\ \ (D^{*+}\to\pi^+D^0) \tag{5}$$

have allowed us to extract a signal without explicitly finding the D^0 decay. Because of the small mass difference

between the $\Upsilon(4S)$ mass and twice the B^0 mass the B mesons are produced nearly at rest in the laboratory. Thus, in a two-body decay to $D^{*+}\pi^-$ both the π^- and the D^{*+} will be nearly monochromatic and anticollinear in momentum. In addition, because of the small energy release in the D^{*+} decay, the slow π^+ from the D^{*+} decay will maintain the direction of the D^{*+}. Events with back-to-back slow and fast pions would then be evidence for this two-body decay. A candidate event is shown in Fig. 12. The actual analysis is described below.

We designate $\vec{p}_s$ and $\vec{p}_h$ as the momenta of the slow and fast pions, respectively; $\vec{p}_s$, $\vec{p}_h$, m_π, and m_D are known. The unobserved momentum $\vec{p}_D$ of the D must be determined in order to measure the invariant mass M_3 of the $D^{*+}\pi^-$ candidates:

$$M_3=[(E_D+E_s+E_h)^2-(\vec{p}_D+\vec{p}_s+\vec{p}_h)^2]^{1/2} . \quad (6)$$

The magnitude of the D^0 momentum $|\vec{p}_D|$ is known, since the B-meson energy $(E_D+E_h+E_s)$ must be equal to the beam energy E_{beam}:

$$|\vec{p}_D|=[(E_{\text{beam}}-E_h-E_s)^2-M_D{}^2]^{1/2} . \quad (7)$$

The two-body invariant mass of the slow π and D must be equal to the D^* mass:

$$M_{D^*}{}^2=(E_D+E_s)^2-(\vec{p}_D+\vec{p}_s)^2$$
$$=M_D{}^2+M_\pi{}^2+2E_DE_s-2\vec{p}_D\cdot\vec{p}_s .$$

Therefore, since

$$\vec{p}_D\cdot\vec{p}_s\equiv|\vec{p}_D||\vec{p}_s|\cos\theta ,$$

we find

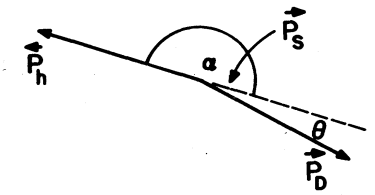

FIG. 13. Vector diagram for the $\bar{B}^0\to D^{*+}\pi^-$ decay.

$$\cos\theta=\frac{M_D{}^2+M_\pi{}^2+2E_DE_s-M_{D^*}{}^2}{2|\vec{p}_D||\vec{p}_s|} . \quad (8)$$

Note also that

$$E_{D^*}=E_D+E_s \quad (9a)$$

and

$$\vec{p}_{D^*}=\vec{p}_D+\vec{p}_s . \quad (9b)$$

We define α to be the measured angle between $\vec{p}_s$ and $\vec{p}_h$ (see Fig. 13), and define ϕ to be the azimuthal angle of $\vec{p}_D$ about $\vec{p}_s$. We cannot determine ϕ but we can choose it so as to maximize the calculated M_3 and thus narrow the apparent mass distribution. The expression for M_3 then translates into a pseudomass

$$(M_{\text{pseudo}})^2=M_{D^*}{}^2+M_\pi{}^2-2E_h{}^2+2E_{\text{beam}}E_h-2p_sp_h\cos\alpha$$
$$-2p_Dp_h(\cos\alpha\cos\theta-\sin\alpha\sin\theta) ,$$

where θ is given by (8). When we select the azimuthal angle in this way, the pseudomass distribution obtained via Monte Carlo simulation of CLEO data (Fig. 14) is narrow, and lies in an interval approximately 14 MeV wide

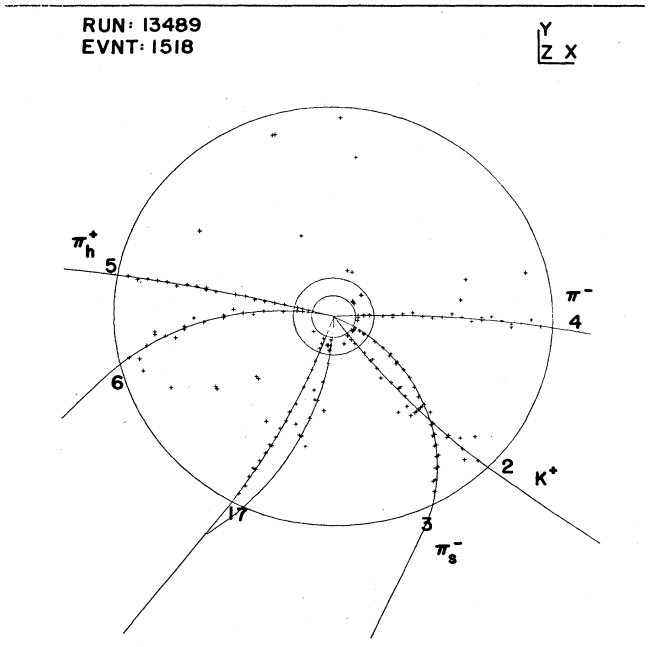

FIG. 12. Candidate event for the decay $B^0\to D^{*-}\pi^+$. The fast pion (π_h^+) and the slow pion (π_s^-) from the D^* decay are indicated as are the decay products of the D^0 which in this rare case is observed to go into $K^+\pi^-$.

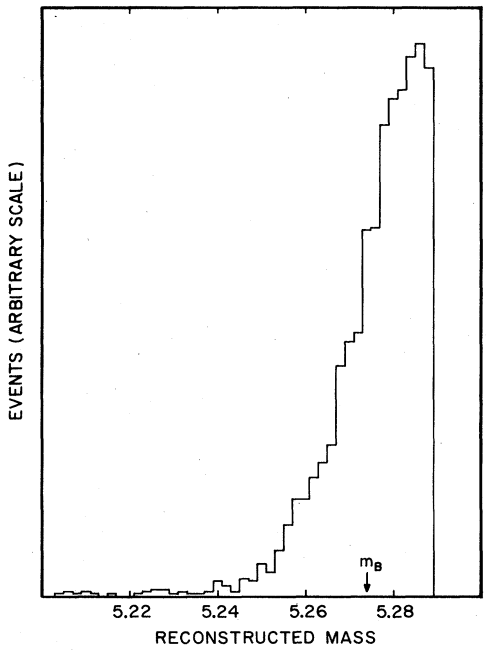

FIG. 14. Monte Carlo distribution for pseudomass calculated for the decay $\bar{B}^0\to D^{*+}\pi^-\to(D^0\pi^+)\pi^-$ using the technique described in the text.

between half the $\Upsilon(4S)$ mass and the true B^0 mass.

Pairs of oppositely charged tracks were considered if they were consistent with a physical $D^*\pi$ state. That is, the energy implied for the D must exceed the D mass, and the minimum pseudomass constructible from the D and π must be less than the D^* mass. In addition we initially required $p_s < 0.25$ GeV/c and $p_h > 2.0$ GeV/c, since we have seen from Monte Carlo simulations that these cuts do not reduce our efficiency. The pseudomass distributions for $\Upsilon(4S)$ and continuum data are shown in Fig. 15. A net signal from $B\bar{B}$ events is evident in the subtracted distribution.

The contribution under the signal peak from continuum events is evaluated by performing the analysis on data taken at energies between the $\Upsilon(3S)$ and $\Upsilon(4S)$ resonances. The reconstructed pseudomass is limited, however, by the beam energy. In order to subtract the continuum contribution properly we set E_{beam} equal to the beam energy at the $\Upsilon(4S)$ and scale the momenta by the mass of the $\Upsilon(4S)$ divided by twice E_{beam}. This provides a reliable means of subtracting the continuum under the $\Upsilon(4S)$ peak, since the momentum distribution of particles from continuum events on and immediately below the $\Upsilon(4S)$ energy is very similar.

There is a contribution to our $D^{*+}\pi^-$ signal from tracks created in the semileptonic B decays $\bar{B}^0 \to D^{*+} l^- \bar{\nu}$ when the lepton (e^- or μ^-) is very fast, and the neutrino is given very little energy. Although the efficiency for this process to produce a signal under our peak is very small, its effect cannot be ignored. The sum of the electron and muon branching ratios[3] for B mesons from the $\Upsilon(4S)$ is $(22.8 \pm 1.4)\%$, much larger than that for the process we hope to investigate. Estimates of the contribution from this source indicate that it could be as high as 20% of our signal, for a cut $p_h > 2.0$ GeV/c. Since the semileptonic branching ratios of charged and neutral B's are not separately known, it is desirable to avoid such a subtraction. The lepton momentum spectrum drops rapidly above 2 GeV/c, so this background is reduced substantially by requiring $p_h > 2.3$ GeV/c.

This particular analysis of $\bar{B}^0$ decay is not overwhelmed by high background levels, despite the lack of full kinematic reconstruction. Since only two tracks are used, the large backgrounds associated with combinatorial juggling of multiple tracks is minimized. In addition, the pool of fast pion candidates is quite small because such energetic particles comprise a very small fraction of the particles generated in $\Upsilon(4S)$ and continuum events.

We have already noted the possible background from semileptonic B decay. Other specific processes which could cause background have been examined and found not to contribute in the signal region. One way of estimating the random background from $B\bar{B}$ events is to invert the three momentum of either pion and repeat the analysis. Since $\vec{p}_s$ and $\vec{p}_h$ should be at roughly 180° relative to each other, the true $\bar{B}^0$ signal does not contribute near the signal peak in the track-inverted analysis. By comparing the distributions obtained from data taken on and below the $\Upsilon(4S)$ (Fig. 16), we conclude that there is no significant contribution to our signal from random combinations in $B\bar{B}$ events. This is not altogether surprising, since there are fewer $B\bar{B}$ events than continuum, and since the $B\bar{B}$ event shape is much less jetlike than in the continuum, pairs of tracks are less likely to occur opposite each other.

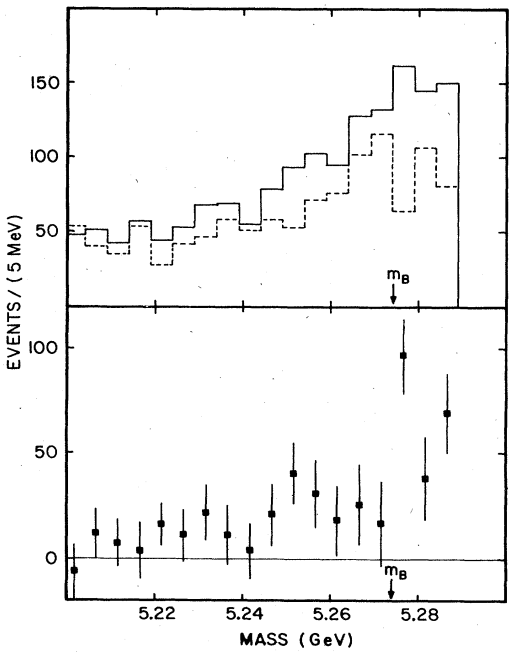

FIG. 15. $D^{*+}\pi^-$ pseudomass distributions using a momentum cut $|\vec{p}_h| > 2.0$ GeV/c. (a) For $\Upsilon(4S)$ (solid line) and continuum (dashed line). (b) Result of continuum subtraction.

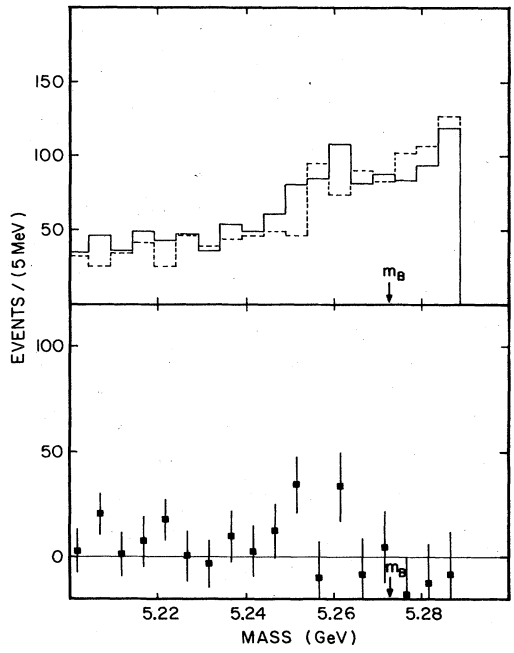

FIG. 16. Track-inverted $D^{*+}\pi^-$ pseudomass distributions using a momentum cut $|\vec{p}_h| > 2.0$ GeV/c. (a) For $\Upsilon(4S)$ (solid line) and continuum (dashed line). (b) Result of continuum subtraction.

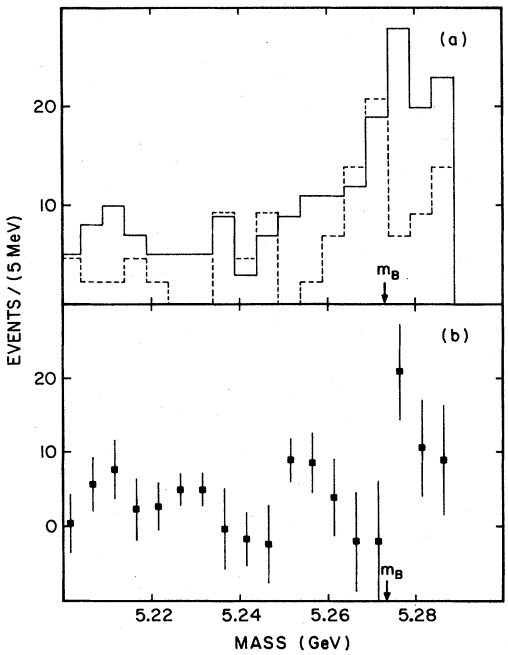

FIG. 17. $D^{*+}\pi^-$ pseudomass distributions using a momentum cut $|\vec{p}_h| > 2.3$ GeV/c. (a) For $\Upsilon(4S)$ (solid line) and continuum (dashed line). (b) Result of continuum subtraction.

To reduce the background from continuum events, we required that the Fox-Wolfram parameter[16] $R_2 = H_2/H_0$ be less than 0.5 for any event containing a candidate. This requirement discriminates against the more jetlike events, so we exclude about 40% of continuum events and lose about 10% of our $\bar{B}^0$ signal. The pseudomass distribution observed for a 2.3-GeV/c momentum cut is shown in Fig. 17. Any candidate with pseudomass $M_{\text{pseudo}} > 5.275$ GeV/c^2 was counted as a $\bar{B}^0$ or B^0. The detection efficiency was estimated, using Monte Carlo events, to be $0.103 \pm 0.004 \pm 0.011$, where the systematic error is due to the uncertainty in the difference between the $\Upsilon(4S)$ mass and twice the B^0 mass. Our analysis yields 71 candidates, which include 30 ± 8 continuum background and 41 ± 12 $\bar{B}^0$ and B^0 candidates. We measure the product of branching fractions

$$B(\Upsilon(4S) \to B^0\bar{B}^0)B(\bar{B}^0 \to D^{*+}\pi^-)B(D^{*+} \to \pi D^0) = 5.0 \pm 1.5 \times 10^{-3} .$$

Assuming that charged and neutral B's are produced in a ratio 6 to 4 (Ref. 17), and that the branching fraction for the decay $D^{*+} \to D^0\pi^+$ is 0.60 ± 0.15 (Ref. 18) we obtain a branching ratio $(2.1 \pm 0.6 \pm 0.5)\%$ for the decay $\bar{B}^0 \to D^{*+}\pi^-$.

D. $D^0\pi^-$ mass plot

We have pursued the $D\pi^-$ final state further. We have looked for events with a D^0 associated with the fast π^-. D^0's were identified by their decay into $K^-\pi^+$. In order to reduce background from continuum two-jet events, we required the cosine of the angle between the π and the $K\pi$ direction in the $K\pi$ rest frame to have an absolute value

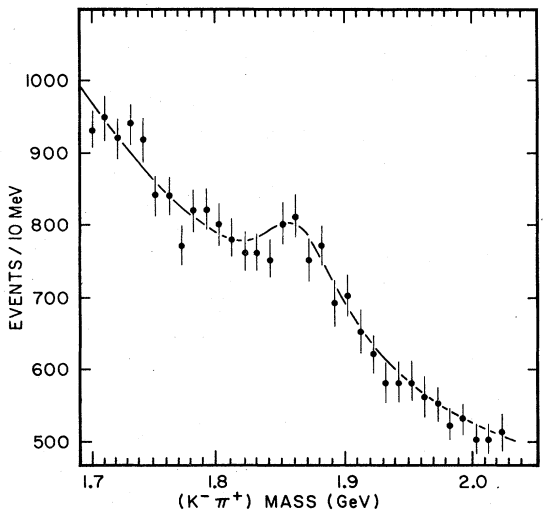

FIG. 18. Invariant-mass combinations of all opposite-sign track pairs interpreted as $K^-\pi^+$ for $\Upsilon(4S)$ events. The momentum of the $K^-\pi^+$ combinations was required to be between 1.5 and 2.8 GeV/c, and the absolute value of the cosine of the angle between the π and the $K\pi$ combination in the $K\pi$ rest frame to be less than 0.8.

of less than 0.8. In order to maximize efficiency, we did not require kaon identification. The resulting $K\pi$ invariant-mass spectrum is shown in Fig. 18 for $K\pi$ momenta between 1.5 and 2.8 GeV/c. D^0 candidates were selected by requiring the $K\pi$ invariant mass to be within 20 MeV of the known D^0 mass. The D^0 energy was recalculated by using the measured K and π momenta and fixing the D^0 mass at 1865 MeV. $D^0\pi^-$ combinations were then examined. Those with energies no less than 0.5 GeV and no greater than 0.25 GeV of the known beam energy were kept. The cut was made asymmetrical to include $D^* \to \pi D^0$ candidates. Since the energy of the B is equal to the energy of the beam, the reconstructed B mass (m_B) is computed from the single-beam energy E_{beam} and the measured momenta $\vec{P}_j$ of the assumed decay products:

$$M_B{}^2 = E_{\text{beam}}{}^2 - \left[\sum \vec{P}_j\right]^2 . \tag{10}$$

The use of the beam energy in Eq. (10), rather than the measured energy improves the resolution in M_B by almost a factor of ten, since the spread in E_{beam} is only 3.2 MeV (rms). In Fig. 19 we show the spectrum in reconstructed B mass for events from the $\Upsilon(4S)$ (solid lines) and an estimate of the background (dashed line). The background

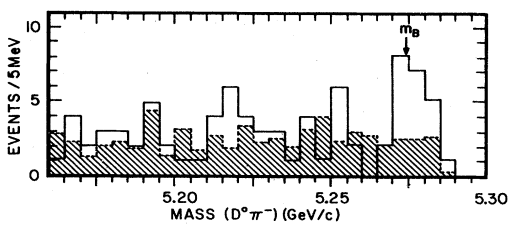

FIG. 19. Reconstructed B mass spectrum for $\Upsilon(4S)$ events (solid histogram) and background estimation (dashed histogram). See text for explanation of background distribution.

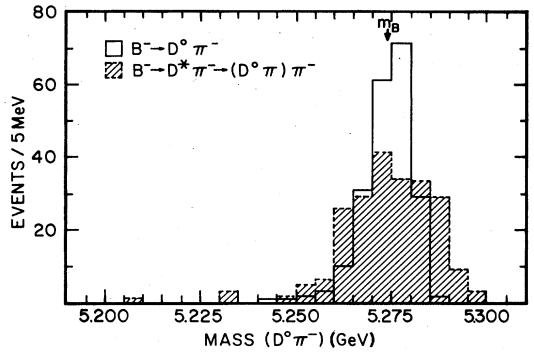

FIG. 20. Monte Carlo distribution of reconstructed B masses for D^0 and D^* final states.

has been determined in three different ways and averaged in order to increase the statistical accuracy. In the first method, the background is measured by taking events in which the pion from the B and the kaon from the D are of opposite charge. This is not allowed for a real B decay since the $b \to c \to s$ decay scheme would be violated. In the second method, we searched for doubly charged D's, either $K^+\pi^+$ or $K^-\pi^-$ and paired them with oppositely charged pions. In the third method mass intervals for D^0 candidates were defined as 20-MeV bands 200 MeV away from 1865 MeV. A clear excess of events above the background appears in the $\Upsilon(4S)$ data sample. We have checked to see if this signal could be the result of other B-meson decay modes, for example, semileptonic decays in which the neutrino is of very low momentum. The semileptonic decays contribute no more than one background event and other processes contribute even less. Then, using the average of the above three background estimates, we find 12.3 ± 5.2 signal events.

The $D^0\pi^-$ final state can result from reactions (1), (2), and (4) listed above, since ignoring the slow pion or soft photon from D^* decay does not significantly alter the B mass reconstructed. In Fig. 20 we show the Monte Carlo–generated reconstructed-B-mass distribution for D^0 and D^* final states. The detection efficiencies, however, do differ. They are listed in Table I.

This result can be expressed in terms of an equation relating the number of events found to a linear combination of branching fractions for reactions (1), (2), and (4). If we assume that the branching fractions are equal, we find that the resulting branching fractions for any one of these channels is $(2.0 \pm 0.8 \pm 0.6)\%$. Here we have assumed that the $\Upsilon(4S)$ decays into B^-B^+ 60% of the time,[17] and have used the measured values $B(D^0 \to K^-\pi^-) = (3.0 \pm 0.6)\%$ (Ref. 19) and $B(D^{*+} \to \pi^+ D^0) = (60 \pm 15)\%$ (Ref. 18). The assumption that B decays to D^* exclusively, i.e., only reactions (2) and (4) are present, leads to a branching ratio of $(4.0 \pm 1.7 \pm 1.0)\%$ for each reaction.

TABLE I. Detection efficiencies for $D^0\pi^-$.

Reaction	Efficiency
$B^- \to D^0\pi^-$	0.20±0.01
$B^- \to D^{*0}\pi^-$ $(D^{*0} \to \pi^0 D^0)$	0.16±0.01
$B^- \to D^{*0}\pi^-$ $(D^{*0} \to \gamma D^0)$	0.14±0.01
$B^0 \to D^{*+}\pi^-$ $(D^{*+} \to \pi^+ D^0)$	0.13±0.01

E. Full B reconstruction

We have also fully reconstructed the $D^{*+}\pi^-$ final state[4] as well as the $D^0\pi^-$ final state. These two-body final states were found along with some three-body final states as described below. Since $b \to c$ dominates, explicit charm signals were first sought. We found D^0's by identifying charged kaons in either the dE/dx or time-of-flight systems and then making mass combinations with all oppositely charged tracks in the event, assuming they were pions. Kaon identification was used to purify the signal. The resulting mass spectrum, shown in Fig. 21, has a peak at the D^0 mass for events from the $\Upsilon(4S)$ and no signal from the continuum. The D^0 momentum range was restricted to be below 2.6 GeV/c, since a D^0 from B decay at the $\Upsilon(4S)$ cannot exceed this momentum, and above 1.0 GeV/c in order to reduce background. We observed charged D^*'s by using the well established trick of computing the $K\pi\pi$-$K\pi$ mass difference, which is known to be 145.4 MeV (Ref. 20) for real $D^{*\pm} \to \pi^\pm D^0$ decay. The resulting $K^\mp\pi^\pm$ mass plot (Fig. 22), for a cut of ± 2.5 MeV around 145.4 MeV, shows a distinct $D^{*\pm}$ signal from the $\Upsilon(4S)$. The data have also been cut on event shape and the decay angle θ of the π in the $K\pi$ rest frame with respect to the $K\pi$ direction in order to enhance the signal. The cuts are $R_2 < 0.3$ and $|\cos\theta| < 0.8$.

Relaxing some of the cuts in order to increase our efficiency, we fit these events with D^0 or $D^{*\pm}$ candidates to the "low-multiplicity" reactions (and their charge conjugates) listed below:

$$B^- \to D^0\pi^- , \tag{11}$$

$$\bar{B}^0 \to D^0\pi^+\pi^- , \tag{12}$$

$$\bar{B}^0 \to D^{*+}\pi^- , \tag{13}$$

$$B^- \to D^{*+}\pi^-\pi^- . \tag{14}$$

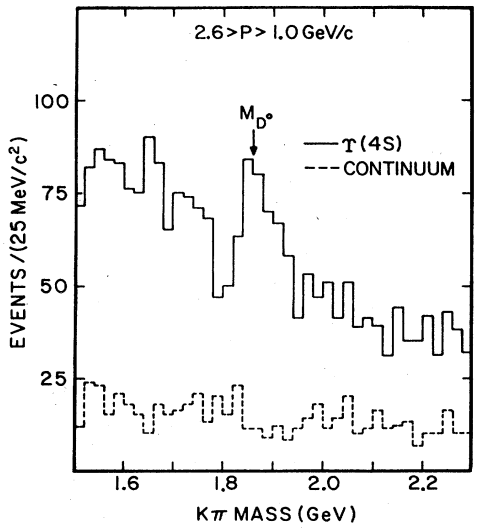

FIG. 21. $K^-\pi^+$ invariant-mass spectrum using kaon identification for events from $\Upsilon(4S)$ (solid line) and continuum (dashed line).

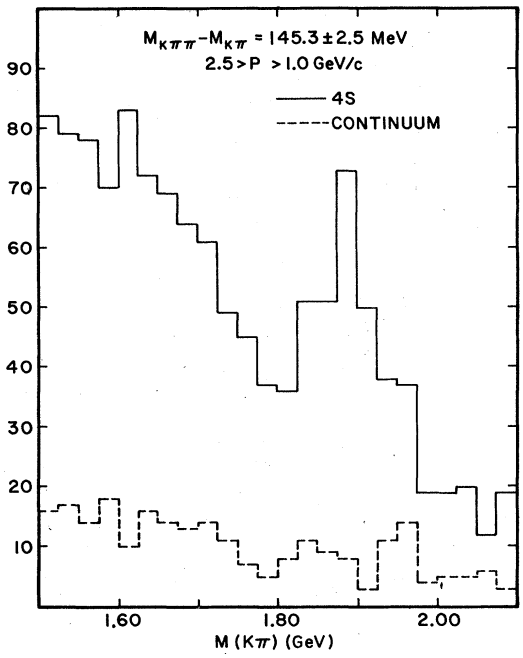

FIG. 22. $K^-\pi^+$ invariant-mass spectrum using $K\pi\pi\pi$-$K\pi$ mass difference cut for events from $\Upsilon(4S)$ (solid line) and continuum (dashed line).

Higher-multiplicity reactions lead to large combinatorial backgrounds. For this analysis D^0 candidates are selected when they have $K^-\pi^+$ masses within 40 MeV of the D^0 mass. For D^{*+} candidates we required the $K\pi\pi-K\pi$ mass difference to be within 3.0 MeV of 145.4 MeV and the $K\pi$ mass to be within 80 MeV of the D^0 mass. There

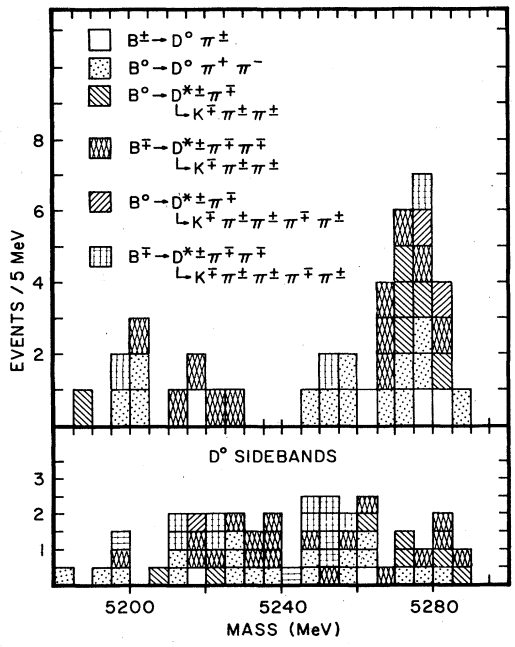

FIG. 23. Reconstructed B-meson spectrum for $\Upsilon(4S)$ events. (a) The D^0 mass cut was taken symmetrically about 1865 MeV. (b) The D^0 mass cut was taken symmetrically about 2065 and 1665 MeV.

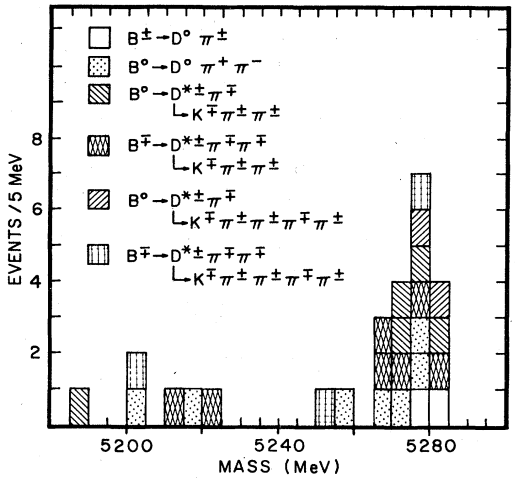

FIG. 24. Reconstructed B-meson mass spectrum for more restrictive cuts in χ^2 and D^0 mass.

was no restriction on R_2 or on $\cos\theta$.

We have also selected charged-D^* decays where the D^0 decays into a K and three charged pions. Here we required the $K\pi\pi\pi\pi$-$K\pi\pi\pi$ mass difference to be within 3.0 MeV of 145.4 MeV and required the $K\pi\pi\pi$ mass to be within 80 MeV of the D^0 mass. We do not search for B's which decay directly to D^0 in the $K\pi\pi\pi$ decay mode because the combinatorial background is too large.

We consider only the above listed charge combinations since they preserve the quark-decay scheme $b\to c\to s$. The fit has two constraints: (1) the energy of the B must equal the beam energy, and (2) the decay products of the D (D^*) must have the right mass. Since the onset of $B\bar{B}$ meson production must occur between the $\Upsilon(3S)$ and $\Upsilon(4S)$ resonances, only B-meson mass combinations between 5.180 GeV and 5.290 GeV were allowed. We required the fit χ^2 be less than 14, taking the hypothesis with the lowest χ^2 when there were ambiguities. The resulting B-meson signal is shown in Fig. 23(a). The width of the peak is 4.5 MeV (rms). The largest contribution to this width is the CESR beam-energy spread of 3.2 MeV. The background was evaluated in several ways. The entire analysis was repeated with the $K\pi$ mass cut displaced by ± 200 MeV from the D^0 mass. The resulting B-mass distribution is shown in Fig. 23(b). The events are plotted with a weight of $\frac{1}{2}$ since there are twice as many events in the sidebands as in the D^0 region. No signal is apparent. The analysis was also repeated off the $\Upsilon(4S)$ peak and no structure was observed. In addition, by narrowing the D^0 mass cuts by 25% and reducing the χ^2 cut to 10, the background is suppressed with little loss of signal (see Fig. 24).

TABLE II. B-mesons masses.

Particle	Mass (MeV)
$\langle B\rangle$	5273.0±1.3±2.0
B^-	5271.2±2.2±2.0
$\bar{B}^0$	5275.2±1.9±2.0
$\bar{B}^0-B^-$	4.0±2.7±2.0

TABLE III. Branching fractions of reconstructed-B-meson channels.

Reaction	Branching fraction (%)
$B^- \to D^0\pi^-$	4.2 ± 4.2[a]
$\bar{B}^0 \to D^0\pi^+\pi^-$	13.0 ± 9.0[b]
$\bar{B}^0 \to D^{*+}\pi^-$	2.6 ± 1.9
$B^- \to D^{*+}\pi^-\pi^-$	4.8 ± 3.0

[a]Includes contribution from $D^{*0}\pi^-$ and $D^{*+}\pi^-$.
[b]Includes contribution from $D^{*0}\pi^+\pi^-$.

Since the energy of the B was constrained to the beam energy, this analysis measures the mass difference between the $\Upsilon(4S)$ mass and twice the B-meson mass. The result is $31.7\pm2.9\pm4.0$ MeV. For mass values we use only the $D^{*\pm}$ final states since the D^0 could result from D^{*0} and thus shift the mass by a few MeV. The mass of the $\Upsilon(4S)$ has been determined by using polarization measurements made now at VEPP-4, CESR, and DORIS.[21] The resulting B masses are given in Table II.

Theoretical predictions for the $\bar{B}^0$-B^- mass difference are of the order of 4 MeV.[22] The CLEO data are not precise enough to test these predictions. The branching fraction of the $\Upsilon(4S)$ to charged or neutral B can be inferred from the measured average B mass with the assumptions (due to Eichten[22]) that the mass difference is 4.4 MeV and that the rates for $\Upsilon(4S)$ to decay to charged or neutral B's differ due to phase space and the effect of the angular momentum barrier. Then the branching fraction for $\Upsilon(4S)\to B^+B^-$ is 0.60 ± 0.02 and the branching fraction for $\Upsilon(4S)\to B^0\bar{B}^0$ is 0.40 ± 0.02.

We now discuss branching-fraction estimates from these fully reconstructed B decays. We do not use the $D^0\to K\pi\pi\pi$ decays in this analysis because we have more events in the corresponding channels where $D^0\to K\pi$. The measured product branching fraction for the $D^{*+}\pi^-$ channel is

$$B[\Upsilon(4S)\to B^0\bar{B}^0]B(\bar{B}^0\to D^{*+}\pi^-)B(D^{*+}\to\pi^+D^0) \times B(D^0\to K^-\pi^+)=2\pm1\times10^{-4}\ .$$

Using the above derived result that the $\Upsilon(4S)$ decays 40% of the time into neutral B's and that $D^{*+}\to\pi^+D^0$ is 60% and $D^0\to K^-\pi^+$ is 3.0%, we arrive at the branching fractions in Table III. The large statistical error as well as large uncertainties in the $D^{*\pm}\to\pi D$ and $D^0\to K\pi$ branching fractions have been added in quadrature.

F. Summary and comparison with theory

In Table IV we summarize the four different measurements of the $B\to D$(or $D^*)\pi^\mp$ branching fraction.

These various measurements show that the branching ratio for the two-body decay $B\to D$ (or $D^*)\pi^-$ is on the order of 2% for any specific decay mode. Unfortunately, the size of the errors precludes any definite conclusion regarding the dominance of D^* versus D final states or the importance of the W exchange diagrams.

The $B\to D\pi^-$ branching fraction can be predicted using the spectator model of b-quark decay. In this section D means the sum of both D and D^* final states. The effective weak Hamiltonian is

$$H=\frac{G}{\sqrt{2}}(J^\mu_+ J_{-\mu}+\text{H.c.})\ , \tag{15}$$

where

$$J^\mu_+=\bar{c}\gamma_\mu(1-\gamma^5)b,\ J_{-\mu}=\bar{u}\gamma_\mu(1-\gamma^5)d\ ,$$

G is the weak-interaction coupling constant, and u, d, c, and b are quark spinors.

The idea is to view the spectator decay of the b quark in two stages, the decay of the b quark to a c quark and a virtual W^-, and the subsequent transformation of the W^- into a π^- meson. We need to assume that the intermediate states in the W^- decay amplitude are saturated by the vacuum, as was done by Tsai in his calculation of τ decays.[23] Since Tsai's predictions agree with the data, this assumption seems well justified. Then, if we assume that the c quark and spectator antiquark system produce only a D, we can write the Hamiltonian as

$$H=\frac{G}{\sqrt{2}}\bar{c}\gamma_\mu(1-\gamma^5)b\langle 0\,|\,A_\mu\,|\,\pi^-\rangle\ . \tag{16}$$

The $\langle 0\,|\,A_\mu\,|\,\pi^-\rangle$ part is measured by $\pi^-\to\mu^-\nu$ decay and is equal to $f_\pi\cos\theta_C\sigma_\mu$, where the pion decay constant $f_\pi=132$ MeV, θ_C is the Cabibbo angle, and q_μ is the pion four-vector. Then the width into $D\pi^-$ is given by

$$\Gamma=\Gamma_0\cos^2\theta_C 12\pi^2\frac{f_\pi{}^2}{m_b{}^2}A\left[\frac{m_c{}^2}{m_b{}^2},\frac{m_\pi{}^2}{m_b{}^2}\right]\lambda\left[\frac{m_D{}^2}{m_B{}^2},\frac{m_\pi{}^2}{m_B{}^2}\right]\ , \tag{17}$$

where

$$\Gamma_0=\frac{G^2 m_b{}^5}{192\pi^3}\,|\,V_{bc}\,|^2$$

(V_{bc} is the b-to-c matrix element),

TABLE IV. $B\to D^\mp$ branching fractions.

Reaction	Method	Value (%)	$D^{*+}\to\pi D$ used	$D^0\to K\pi$ used
(1) $B\to D^0\pi^-$, $D^{*0}\pi^-$, $D^{*+}\pi^-$, $D^+\pi^-$	Fast-π momentum spectrum	$2.0\pm0.6\pm0.5$	No	No
(2) $B\to D^0$ (or D^0 and $D^*)\pi^-$	$D^0\pi^-$ mass plot	$2.0\pm0.8\pm0.6$	No	Yes
(3) $B^0\to D^{*+}\pi^-$	Slow-π–fast-π	$2.1\pm0.6\pm0.5$	Yes	No
(4) $B^0\to D^{*+}\pi^-$	Reconstruction	2.6 ± 1.9	Yes	Yes

TABLE V. Predicted two-body B branching ratios.

Decay mode	Branching ratio (%)
$D\pi^-$	1.9
DF^-	3.8 $(f_F/0.240)^2$
DK^-	0.2
$D\rho^-$	4.9
DF^{*-}	5.3 $(f_{F^*}/0.240)^2$
DK^{*-}	0.2

$$A(x,y)=(1-x^2)-y(1+x)\ ,$$

$$\lambda^2(x,y)=(1-x-y)^2-4xy\ .$$

In the case in which the virtual W transforms into a vector meson V the formulas change to

$$H=\frac{G}{\sqrt{2}}\bar{c}\gamma_\mu(1-\gamma^5)b\langle 0\,|\,V_\mu\,|\,V^-\rangle\ , \tag{18}$$

$$\Gamma=\Gamma_0\cos^2\theta_C 12\pi^2\frac{f_V{}^2}{m_b{}^2}B\left[\frac{m_c{}^2}{m_b{}^2},\frac{m_V{}^2}{m_b{}^2}\right]\lambda\left[\frac{m_D{}^2}{m_B{}^2},\frac{m_V{}^2}{m_B{}^2}\right]\ , \tag{19}$$

where

$$B(x,y)=(1-x-y)(1+x-2y)-4x\ ,$$

and f_V is the vector-meson decay constant. If the vector-meson coupling is Cabibbo suppressed, the $\cos^2\theta_C$ factor is replaced by $\sin^2\theta_C$.

These rates are changed by strong-interaction corrections due to gluon exchanges which in leading-logarithm approximation increase the width by 11%.[2] W-exchange diagrams may contribute in $\bar{B}^0$ decay and would also change the decay rate. These exchanges are not expected to account for more than 15% of the total width,[2] but may affect specific two-body processes differently. Ignoring this contribution we arrive at the predicted rates given in Table V.

This model is in good agreement with our data for $D\pi^-$. An earlier model of Ali, Körner, Kramer, and Willrodt,[24] which treats the W^- vertex differently, also arrives at an approximate 2% rate for $B\to D^*\pi^-$.

IV. SEARCH FOR TWO-BODY DECAYS RESULTING FROM $b\to u$ TRANSITIONS AND TWO-BODY DECAY INTO CHARGED LEPTONS

A. $\bar{B}^0\to\pi^+\pi^-$ and $B^-\to\rho^0\pi^-$

Weak decay of the b quark into the u quark rather than the c quark would manifest itself by B-meson decay into final states without a charmed particle. In the spectator model the b quark decays into a virtual W^- and a u quark. The spectator quark then combines with the outgoing quarks and forms hadrons. In addition, the $b\to u$ transition can occur via a W-exchange graph (for $\bar{B}^0$) or via an annhilation graph into W (for B^-). We have searched for the final states $\pi^+\pi^-$ from $\bar{B}^0$ decay and $\rho^0\pi^-$ from B^- decay.

For the $\bar{B}^0\to\pi^+\pi^-$ hypothesis we required the energy of the $\pi^-\pi^+$ pair to be within 300 MeV of the known beam energy ($E_{\rm beam}$). For the $B^-\to\rho^0\pi^-$ hypothesis we required the energy of the $\rho^0\pi^-$ combination to be within 250 MeV of $E_{\rm beam}$. We defined the ρ^0 as any $\pi^+\pi^-$ pair with invariant mass between 0.5 and 1.0 GeV. In each case the mass of the B-meson candidate was calculated using the known beam energy through Eq. (10). In Fig. 25 we show the distribution of $(M_B-E_{\rm beam})$ for $\Upsilon(4S)$ and continuum for each decay mode. The background in these distributions is large. In this section we discuss some ideas which have enabled us to reduce the background.

The two-body final states we are considering here have the outgoing particles at large momentum in order to sum to the beam energy, and yet have relatively low total momentum (400 MeV/c). Thus they are almost oppositely directed in the laboratory. Since B decays produce few high-momentum particles, and the particles in these final states have the maximum allowed momentum, the background comes mainly from continuum events. Therefore, we expect the background events to have two-jet structure. We now demonstrate that backgrounds to the B decays considered here occur when one of the two final-state particles is in one jet and the other in the opposite jet. First, for each event we found the jet axis[25] of the remaining particles with the candidate B decay removed. We then found the cosine of the angle between the final-state particles (π or ρ) and this jet axis ($\cos\theta$). Figure 26 shows the $\cos\theta$ distributions for each decay mode for the continuum data. A strong angular correlation exists between the fast particles and the jet axis of the remaining particles. In contrast, Fig. 27 shows the same distributions for Monte Carlo events in which the $\bar{B}^0$ (B^-) decays into $\pi^+\pi^-$ ($\rho^0\pi^-$) and the other B^0 (B^+) decays normally, that is essentially isotropically. As expected, there is hardly any angular correlation. In order to reduce the background, we rejected combinations if $|\cos\theta|$ for at least one of the

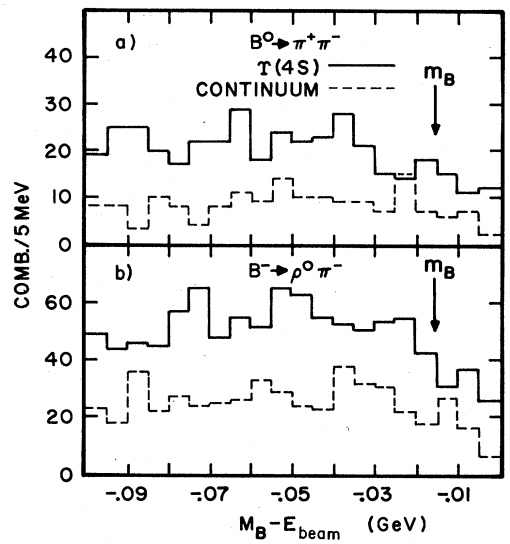

FIG. 25. $(M_B-E_{\rm beam})$ distributions. (a) $B^0\to\pi^+\pi^-$, (b) $B^-\to\rho^0\pi^-$.

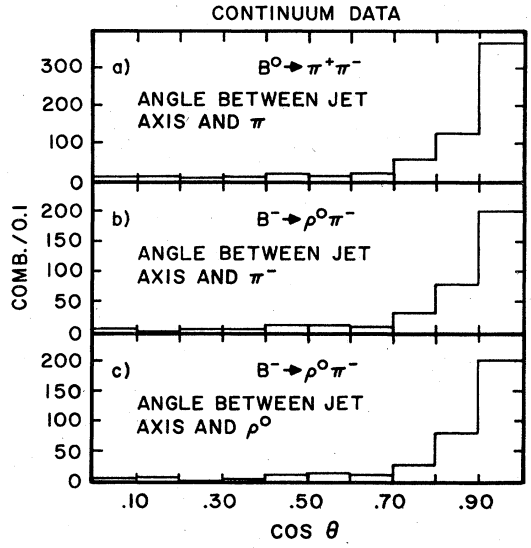

FIG. 26. $|\cos\theta|$ for the continuum data sample. (See text for definition.) (a) π from $B^0 \to \pi^+\pi^-$, (b) π from $B^- \to \rho^0\pi^-$, (c) ρ from $B^- \to \rho^0\pi^-$.

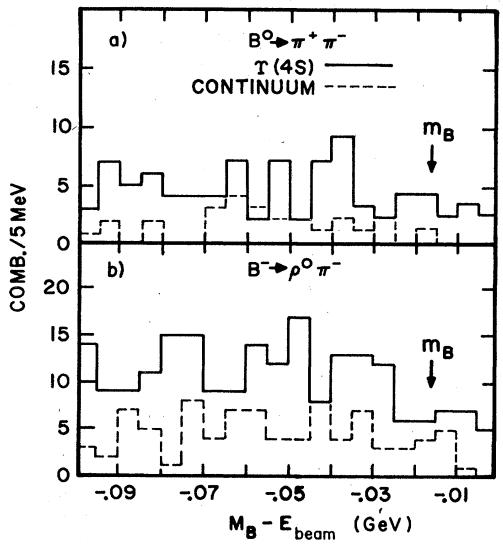

FIG. 28. $(M_B - E_{beam})$ distributions cut on $|\cos\theta| < 0.8$ and polarization cut on ρ. (a) $B^0 \to \pi^+\pi^-$, (b) $B^- \to \rho^0\pi^-$.

fast particles was greater than 0.8. This reduces the acceptance by about 20%.

Since the ρ in $B^- \to \rho^0\pi^-$ is polarized in the helicity 0 state, we can further reduce the background for this decay mode. We define a polarization angle θ_π in the following way. First, find the direction of ρ in the B rest frame. Then, find the direction of the π^+ in the ρ rest frame. θ_π is the angle between these two directions. Because of the polarization, only 25% of the Monte Carlo signal events have $|\cos\theta_\pi|$ less than 0.5, whereas the background is flat as a function of $\cos\theta_\pi$. Therefore we eliminate events with $|\cos\theta_\pi|$ less than 0.5.

Figure 28 shows the distribution of $M_B - E_{beam}$ with the cuts described above, for both the $\Upsilon(4S)$ and continuum data samples. In Fig. 29 the continuum data have been subtracted. We examine the two mass bins which would be populated with B-meson events, namely, -10 MeV $> M_B - E_{beam} > -20$ MeV. No signal appears. In the two mass bins of interest, we find 3.7 ± 3.5 $\pi^+\pi^-$ candidate events and in the $\rho^0\pi^-$ mass plot we find -7.8 ± 7.9 events. These numbers translate into 90%-confidence-level upper limits of 8.5 events for $B^0 \to \pi^+\pi^-$ and 9.1 events for $B^- \to \rho^0\pi^-$. We estimated the detection efficiency for each decay mode using Monte Carlo events to be 50 and 31%, respectively. We have 42 000 $B\bar{B}$ pairs. Assuming a 6:4 ratio of B^- to B^0, these results correspond to branching-ratio upper limits of 0.05% for $B^0 \to \pi^+\pi^-$ and 0.06% for $B^- \to \rho^0\pi^-$.

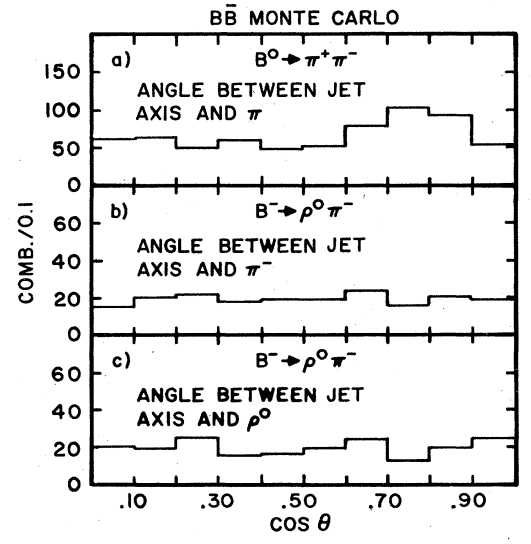

FIG. 27. $|\cos\theta|$ for $B\bar{B}$ Monte Carlo data. (See text for definition.) (a) π from $B^0 \to \pi^+\pi^-$, (b) π from $B^- \to \rho^0\pi^-$, (c) ρ from $B^- \to \rho^0\pi^-$.

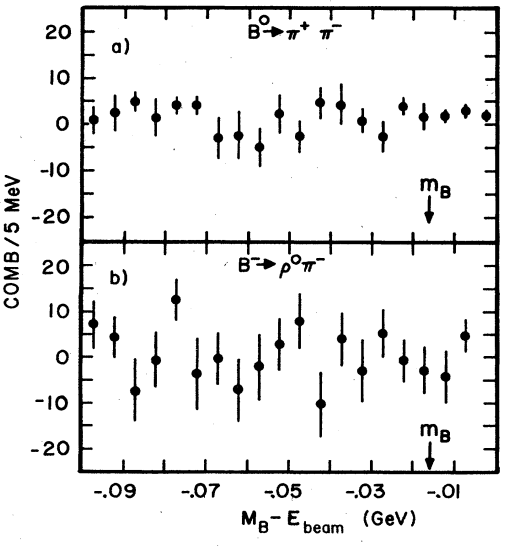

FIG. 29. $(M_B - E_{beam})$ distributions for $\Upsilon(4S)$ data continuum subtracted with cuts on $|\cos\theta| < 0.8$ and polarization cut on ρ. (a) $B^0 \to \pi^+\pi^-$, (b) $B^- \to \rho^0\pi^-$.

We do not know what branching ratio to expect for these final states. The upper limit on $(b\to u)/(b\to c)$ obtained using semileptonic B decays[3] is 4%. If the fraction of $b\to u$ that goes into any one of these final states were 2%, and $(b\to u)/(b\to c)$ were 4%, then the branching ratio for the final states considered here would be 0.08%. Thus, the limits found here are not trivial, although it is not possible to translate them directly into an upper limit on inclusive $b\to u$ decays in a model-independent way.

B. Search for exclusive $\bar{B}^0$ decays into two charged leptons

Our search for the $\pi^+\pi^-$ final state is not sensitive to the mass of the final-state particles, provided that they are light, since the mass enters only in the energy constraint. Therefore, the upper limit of 0.05% applies for any final-state particles with a pion mass or less. When the final-state particles are leptons the limits are improved by using the lepton identification capabilities of the CLEO detector.[14] For the decay $\bar{B}^0\to\mu^+\mu^-$, we improve our limit by requiring that both muons penetrate the iron and produce signals in drift chambers. We find no such events. After correcting for detection efficiency (33%), we set an upper limit of 0.02% at 90% confidence for this decay. We improve our limit for $\bar{B}^0\to e^+e^-$ by requiring that only one of the electrons be positively identified in the dE/dx and shower-chamber systems. One found candidate, coupled with a detection efficiency of 33%, gives a 90%-confidence-level upper limit of 0.03%. Finally, for the decay $\bar{B}^0\to\mu^\pm e^\mp$, we require the muon to be identified but the electron needs to be positively identified if it is in the fiducial volume of the electron detectors. This procedure gives an efficiency of 42%. The two candidate events found give an upper limit at 90% confidence level of 0.03%.

V. CONCLUSIONS

Hadronic B decays have a mean charged multiplicity of 6.0 ± 0.3 and semileptonic B decays have a mean charged multiplicity of 3.8 ± 0.4. The two-body branching fractions of $B\to D\pi^-$ have been measured in four different ways and give values of about 2%. Inclusive ψ decay accounts for no more than 1.6% of B decay (at the 90% confidence level), and thus demonstrates the suppression of color mixing in B decays. The branching fractions for $B^-\to\psi K^-$ and $\bar{B}^0\to\psi K^-\pi^+$ are less than 0.26% and 0.63%, respectively. The noncharmed final states $\pi^+\pi^-$ and $\rho^0\pi^-$ have also not been observed. The upper limits (90% confidence level) are 0.05% and 0.06%, respectively. This is consistent with a small $b\to u$ coupling.

Theoretical predictions using the standard electroweak model with QCD corrections are consistent with the data. The data are consistent with a model where the B decays into a D and virtual W, the virtual W then transforming into hadrons or leptons in the case of semileptonic B decay or into a pion in the case of two-body B decay. Although this picture probably will not explain all of B decay, it provides a starting point for understanding most of B decay.

ACKNOWLEDGMENTS

This work could not have been undertaken without the dedicated efforts of the CESR staff, for which we are most grateful. This work was partially supported by both the National Science Foundation and the Department of Energy.

---

*Permanent address: LPC, College de France, Paris 75231 Cedex 05, France.
†Present address: University of Oklahoma, Norman, OK 73019.
‡Present address: Indiana University, Bloomington, IN 47405.
§Present address: EP Division, CERN, CH-1211 Geneva 23, Switzerland.

[1]J. Ellis, M. K. Gaillard, D. V. Nanopoulos, and S. Rudaz, Nucl. Phys. B131, 285 (1977); M. Kobayashi and T. Maskawa, Prog. Theor. Phys. **49**, 652 (1973).
[2]See H. Fritzsch, Phys. Rep. **73**, 68 (1981); R. Rückl, Habilitationschrift submitted to University of Munich, 1983 (unpublished).
[3]A. Chen *et al.*, Phys. Rev. Lett. **52**, 1084 (1984); C. Klopfenstein *et al.*, Phys. Lett. **130B**, 444 (1983).
[4]S. Behrends *et al.*, Phys. Rev. Lett. **50**, 881 (1983).
[5]D. Andrews *et al.*, Phys. Rev. Lett. **45**, 219 (1980); G. Finnocchiaro *et al.*, *ibid.* **45**, 222 (1980).
[6]D. Andrews *et al.*, Nucl. Instrum. Methods **211**, 47 (1983); R. Ehrlich *et al.*, *ibid.* **211**, 17 (1983).
[7]J. Green *et al.*, Phys. Rev. Lett. **51**, 347 (1983).
[8]A. Ali, Z. Phys. C **1**, 25 (1979). The decay corresponds to model I.
[9]M. S. Alam *et al.*, Phys. Rev. Lett. **49**, 357 (1982).
[10]We have assumed a $B\to\tau+X$ branching fraction of 2%.
[11]H. Fritzsch, Phys. Lett. **86B**, 164 (1979); **86B**, 343 (1979).
[12]J. H. Kühn, S. Nussinov, and R. Rückl, Z. Phys. C **5**, 117 (1980); T. DeGrand and D. Toussaint, Phys. Lett. **89B**, 256 (1980); M. B. Wise, *ibid.* **89B**, 229 (1980).
[13]J. H. Kühn and R. Rückl, Phys. Lett. **135B**, 477 (1984).
[14]K. Chadwick *et al.*, Phys. Rev. D **27**, 475 (1983).
[15]If there is an excited D^* state close to the D^* mass of 2009 MeV, we would include it in our definition of D^*.
[16]Geoffrey C. Fox and Stephen Wolfram, Phys. Rev. Lett. **41**, 1581 (1978). The variable R_2 is defined as $R_2=H_2/H_0$, where

$$H_l=s^{-1}\sum_{ij}|p_i||p_j|P_l(\cos\theta_{ij})\ .$$

Here p_i and p_j are the momenta of particles i and j, P_l is the lth Legendre polynomial, and θ_{ij} is the angle between particles i and j.
[17]The reasons behind this assumption are explained later in Sec. III E.
[18]G. Goldhaber *et al.*, Phys. Lett. **69B**, 503 (1977). The value quoted here is 0.60 ± 0.15 for $D^{*+}\to D^0\pi^+$. CLEO uses this value rather than a more recent value of 0.44 ± 0.10 from W. Coles *et al.* [Phys. Rev. D **26**, 2190 (1980)], because the latter did not assume isospin conservation among the strong decays of the D^{*+} and their reported values are somewhat incon-

sistent with this assumption.
[19]R. H. Schindler *et al.*, Phys. Rev. D **24**, 78 (1981).
[20]Particle Data Group, Phys. Lett. **111B**, 1 (1982).
[21]B. Gittelman, in *Proceedings of the 1983 International Symposium on Lepton and Photon Interactions at High Energies, Ithaca, New York,* edited by D. G. Cassel and D. L. Kreinick (Newman Laboratory of Nuclear Science, Cornell University, Ithaca 1983).
[22]E. Eichten, Phys. Rev. D **22**, 1819 (1980). Other authors have found different values: see Lai Him-Chan, Phys. Rev. Lett. **51**, 252 (1983).
[23]Y. S. Tsai, Phys. Rev. D **9**, 2821 (1971).
[24]A. Ali, J. G. Körner, G. Kramer, and J. Willrodt, Z. Phys. C **1**, 269 (1979).
[25]The jet axis is defined as the axis which minimizes

$$S=\frac{3}{2}\frac{\sum_k |\vec{p}_{kt}|^2}{\sum_k |\vec{p}_k|^2} .$$

The $\vec{p}_{kt}$ appearing in the equation are the transverse momentum components, taken with respect to the chosen axis. The k index runs over the final-state particles.